Proceedings of the 2010 3rd IEEE RAS & EMBS
International Conference on Biomedical Robotics and Biomechatronics,
The University of Tokyo, Tokyo, Japan, September 26-29, 2010

Development of a Myoelectric Joystick: a Preliminary Study

Changmok Choi, *Student Member, IEEE,* and Jung Kim, *Member, IEEE*

***Abstract*—Current manual joysticks have been widely used to control various artificial devices, but they are expensive and composed of mechanically bulky frames. To address these issues, we developed a myoelectric joystick using surface electromyogram (sEMG) from six muscles that make a wrist joint move. Fluid wrist movements were estimated by introducing a non-negative muscle synergy matrix and a joint synergy matrix. Only four movements were predefined (wrist extension, wrist flexion, radial deviation, and ulnar deviation) to construct the muscle synergy matrix, but an experimental result showed that a variety of movements (e.g., a combination of wrist extension and ulnar deviation) could be extracted using the joint matrix. This work also could be extended for development of an alternative computer interface and powered wrist prosthesis for individuals with transradial or wrist disarticulation level amputation.**

I. Introduction

A manual joystick has been used to control a variety of artificial devices in many industrial and home applications, such as assembly lines, video games, and aircrafts. This device consists of a stick that pivots on a base and reports its angle and direction. The reported information represents a two-dimensional Euclidean vector that consists of a direction and a magnitude. Due to the bulky frame and high cost of the joystick, there have been attempts to suggest an alternative joystick by capturing hand gestures from sEMG [1].

SEMG is the electrical representation of activities produced by a number of muscle fibers in a contracting muscle. This electrical representation reflects the degree of the muscle activation: the higher the sEMG level, the greater the muscle force is developed. Most work using sEMG has come out for the development of the prosthesis [2], but recently much research has been carried out for other applications: teleoperation [3], exoskeleton [4], computer interface [5], and human-assisting manipulation [6].

There are three advantages of using sEMG to alternate the conventional joystick. First, a mechanically bulky frame is not required and a sEMG sensor is cheap. Second, no additional mental load is required to produce sEMG because the sEMG is naturally accompanied by body movements (perhaps even unconsciously). Third, mobile computing is possible because the sEMG sensor is light and wearable.

There have been myriad methods to classify wrist movements via sEMG using machine learning algorithms: artificial neural networks [5], support vector machines [7], Bayesian networks [8], the Gaussian mixture model classifier [9], and a hidden Markov model [10]. Most proposed methods can extract only a static gesture (ON/OFF) of predefined wrist movements. Therefore, directions of the movements are limited and a proportional controllability is absent.

In this paper, we proposed a myoelectric joystick by extracting wrist movements using a non-negative muscle synergy matrix and a joint synergy matrix. We selected wrist movements for the joystick inputs because the wrist is a mechanically universal joint, movements of which are similar to those of the conventional joystick. A non-negative muscle synergy matrix was introduced to transform six muscle activities into four predefined wrist movements (wrist extension, wrist flexion, radial deviation, and ulnar deviation) as shown in Fig. 1. The directions of the predefined movements were constrained only to the two axes that are

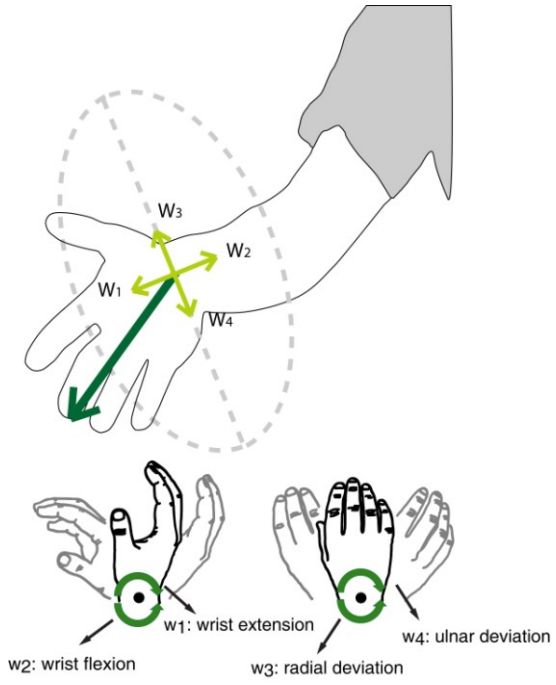

Fig. 1. Four representative wrist movements.

Manuscript received April 9, 2010. This work was supported by the Korea Science and Engineering Foundation (KOSEF) funded by the Korea government (MOST) under Grant R01-2007-000-11659-0.

C. Choi is with the Department of Mechanical Engineering, Korea Advanced Institute of Science & Technology (KAIST), Daejeon, Republic of Korea (e-mail: axlguitar@kaist.ac.kr).

J. Kim is with the Department of Mechanical Engineering, Korea Advanced Institute of Science & Technology (KAIST), Daejeon, Republic of Korea (corresponding author to provide phone: +82-42-350-3271; fax: +82-42-350-5230; e-mail: jungkim@kaist.ac.kr).

978-1-4244-7707-4/10/$26.00 ©2010 IEEE

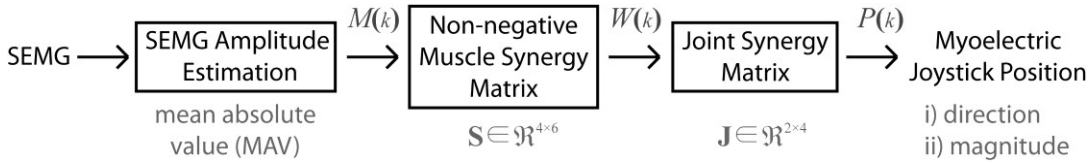

Fig. 2. A block diagram for the myoelectric joystick.

perpendicular in two-dimensional space. Therefore, each movement spanned only a one dimensional space. A joint synergy matrix was formulated to span the whole two-dimensional space by combining four predefined wrist movements.

II. Materials and Methods

A. System Overview

Figure 2 shows a block diagram for the myoelectric joystick. We selected six muscles of the forearm to record sEMG: 1) extensor carpi radialis (ECR), 2) abductor pollicis longus (APL), 3) flexor carpi radialis (FCR), 4) flexor carpi ulnaris (FCU), 5) extensor carpi ulnaris (ECU), and 6) extrinsic digital extensors (EDE). These muscles are responsible for the four wrist movements (wrist extension, wrist flexion, radial deviation, and ulnar deviation).

We placed bipolar, noninvasive surface electrodes (DE-2.1, Delsys, U.S.A.) with built-in amplifiers using medical adhesive tape over the target muscles. The electrodes were connected to a data acquisition board (PCI 6224, National Instruments™, U.S.A.), and the signals were sampled at 1000 Hz. To quantitatively estimate the muscle activities from sEMG, we used mean absolute value (MAV) that has been widely used because of the probabilistic nature of sEMG magnitudes [11].

It has been generally accepted that the central nervous system simplifies control of movements through a hierarchical and modular architecture, and this strategy is regarded as an effective way to circumvent the difficulty of controlling many degrees of freedom in the musculoskeletal apparatus [12]. At the lowest level of the hierarchy, muscle recruitment might be controlled by a small number of functional units, thereby reducing dimensionality of output space. Higher levels in the hierarchy might recruit and flexibly combine these output modules to control a variety of different movements. Several researchers have provided evidence that the basic control modules allow for the generation of appropriate muscle patterns through simple modulation and combination rules [13]. We defined output modules to simplify mapping between the muscular activities and each wrist joint movement. The output modules were combined to extract fluid joint movements (direction and magnitude).

B. Non-negative Muscle Synergy Matrix

We constrained the synergy matrix as none of the components in the mapping matrix was negative. Synapses in a biological neural network are either excitatory or inhibitory but always send a signal rather than retracting one. For instance, if an agonist movement appears after its antagonist movement, agonist muscles should be excitatory and antagonist muscles should be inhibitory. To make agonist muscles excitatory, firing rates of neurons should increase. In contrast, to make antagonist muscles inhibitory, firing rates of neurons should decrease. Therefore, the non-negativity of the hidden and visible variables corresponds to the physiological fact that the firing rates of neurons cannot be negative. In a similar sense, we defined agonist and antagonist movements as having different synergies, although they could share the same DOFs (e.g., wrist extension and wrist flexion). The non-negativity characteristic in the synergy matrix does not directly allow an agonist muscle activation to decrease an antagonist movement, or vice versa. For an agonist movement, the magnitude of agonist muscle activations should be greater than the magnitude of antagonist muscle activations in the proposed matrix. This is in agreement with scientific understanding of how the joint movements of the human limb work with agonist and antagonist muscles.

The output module was defined from six muscular activities to one (d-direction) of the predefined wrist movements as a row vector

$$S_d = \left[s_{d,1}, \quad s_{d,2}, \ldots, \quad s_{d,5}, \quad s_{d,6} \right]. \tag{1}$$

A group of the muscular activities was defined as a column vector $M(k)$ that produced a wrist joint movement $w_d(k)$ in the d-direction based upon the output module.

$$W_d(k) = S_d \times M(k), \quad d = 1, \cdots, 4. \tag{2}$$

$W_{1\text{-}4}(k)$ represents wrist extension, wrist flexion, radial deviation, and ulnar deviation from its neutral position, respectively.

C. Supervised Optimization

If $M(k)$ and $W(k)$ are sampled while moving a wrist joint during K discrete time intervals, the wrist movements can be expressed as a product of **S** times **M**.

$$\mathbf{W} \approx \mathbf{S} \times \mathbf{M} \tag{3}$$

where **W** is a matrix consisting of $W(k)$ over the total samples and has 4 rows and K columns (K is the total number of samples). **M** is a matrix consisting of $M(k)$ over the total

samples and has L rows and K columns (L is the number of the muscles involved in producing the wrist movements). To find an approximate optimal matrix **S**, we first needed to define a cost function that quantifies the quality of the approximation. The cost function was defined as follows:

$$Minimize\ E = \frac{1}{2}\left\|\mathbf{W} - \mathbf{S}\times\mathbf{M}\right\|^2 \ with\ respect\ to\ \mathbf{S} \quad (4)$$

$$, subject\ to\ the\ constraints\ \mathbf{S} \geq 0.$$

We used an additive update rule to find the optimal **S** that reduces the cost function and can be written as:

$$s_{d,l} \leftarrow s_{d,l} - \eta\frac{\partial E}{\partial s_{d,l}}, \quad (d = 1,\cdots,4\ \&\ l = 1,\cdots,L) \quad (5)$$

$$\frac{\partial E}{\partial s_{d,l}} = \sum_{k=1}^{K}\left\{\left(w_d(k) - \sum_{l=1}^{L} s_{d,l}\times m_l(k)\right)\cdot\left(-m_l(k)\right)\right\} \quad (6)$$

where η is a small positive number. Iteration of these update rules converges to a local minimum of the cost function. To constrain the non-negativity of elements in the matrix **S**, the updated elements which have negative signs change to zero at each iteration. It could be argued whether constraint of non-negative numbers leads to the convergence. Even though we constrained a range of elements in the matrix **S**, this constrains does not change the mean-square error surface defined by equation (4). Therefore, this optimization process with non-negativity constraints leads to the convergence to find the optimal matrix **S**.

D. Joint Synergy Matrix

The position of a prosthetic wrist is denoted as a column vector $P(k)$ in a two-dimensional Cartesian space. The joint synergy matrix **J** is supposed to map between wrist movement intents and position of the prosthetic wrist. $p_x(k)$ represents flexion-extension and $p_y(k)$ represents radial-ulnar deviation. In this regard, the matrix **J** is constructed:

$$\mathbf{J} = \begin{bmatrix} 1 & -1 & 0 & 0 \\ 0 & 0 & 1 & -1 \end{bmatrix}. \quad (7)$$

III. EXPERIMENT

A. Subjects

Four male (Subjects A-D) and one female (Subject E) volunteers with an average age of 22.8 years (SD 1.9) took part in our experiments. The KAIST Institutional Review Board approved the experimental protocol and the publication of this study (File No. KH2008-3). All participants reported no history of upper extremity or other musculoskeletal complaints, and participants were fully informed of the details of the experimental procedure.

B. Experimental Setup

Subjects were requested to sit comfortably on a chair, while sEMG sensors were attached on the forearm. Subjects could control the position of a control cursor (blue) on the screen via their wrist movements and were requested to place the control cursor on a target cursor.

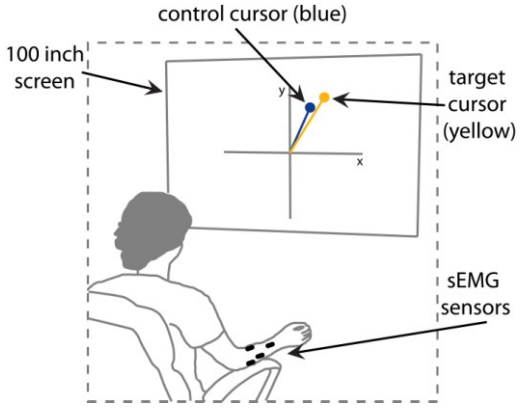

Fig. 3. Experimental setup.

We used a personal computer (Pentium 4, 2.4 GHz processor) with a graphics card (NVIDIA GeForce 8600 GT). The source code was written in Microsoft Visual Studio 2005. The OpenGL library was used for graphics rendering, and an update of 40 Hz for the graphics loop was achieved. The visual graphic engine projected the visual representation of cursors via a beam projector (NP-2000, NEC, U.S.A.) with a 100-inch screen as shown in Fig. 3.

The origin of the coordinate was defined as the center of the visual display, and $p_x(k)$ and $p_y(k)$ were scaled by 400 pixels for visualization on a screen. The $P(k)$ was displayed as a line on the screen, and at the end of the line, a circle cursor was drawn. Therefore, the cursor represents the direction of wrist movements from the origin (neutral position), and the length of the line represents intensities of the movements.

C. SEMG Amplitude Estimation

For the real-time use of MAV, there is a trade-off between the responsiveness (rapid detection of onset or offset of muscle activation) and signal-to-noise ratio (SNR, in which the noise is defined as a variability in sEMG by Clancy [14]). When we use a large time window for MAV, it reduces not only variability in sEMG but also the rapid change, which could be intentional muscle activation. In addition, since MAV is a casual signal processor, this large time window introduces a significant delay. When we use a short window to reduce the delay effect, it increases the signal variability in sEMG. This trade-off has been reported in literature [15]; recently, there have been efforts to increase both SNR and responsiveness in sEMG estimations [16].

For the sEMG amplitude estimation in our experiment, a MAV with a 500-msec window was used. It could be argued that a 500-msec window used in this experiment was too long to catch rapid response of muscle activation. The window length was selected based on pilot studies. When the window length was set below 500 msecs, the control cursor by sEMG highly fluctuated, so we found subjects were unable to easily

catch the target and sometimes suffered from serious eyestrain. Therefore, we believe that the experimental protocol with shorter window length would not be helpful to verify the feasibility of a non-negative muscle synergy matrix. In a similar sense, we avoided using a small (19-inch) computer monitor, because we found subjects suffered from eyestrain. Using a 100-inch screen with a beam projector made subjects feel more comfortable, probably as a consequence of the distance between the subjects and the screen.

D.Experimental Protocol

The experiment consisted of 15 sessions in total, each consisting of one training and three tests. In the training, a target cursor (yellow) was displayed on the screen in two dimensions, as shown in Fig. 3; the displayed trajectories are shown in Fig. 4. While displaying the target cursor, subjects were asked to proportionally move their wrist towards the position of the target from the center of the screen. When the target was positioned at (0, 0) in the (X, Y) coordinate, the subjects held their wrist in the neutral position. When the target was positioned at (400, 0), the subjects fully extended the wrist. In a similar sense, (-400, 0), (0, 400), and (0, -400), the positions of the target represented full wrist flexion, full radial deviation, and full ulnar deviation, respectively. When the target gradually moved between the center and outer position on the screen, the subjects were asked to voluntarily modulate levels of wrist movements between full activation and no activation, according to the position of the target. During the training, the smoothed sEMG and target positions were recorded at 1000 Hz and stored in matrices **M** and **W**, respectively, as shown in Equation (3). In the matrix **M**, the stored data in each row represents the smoothed sEMG from each single channel and these data were normalized from 0 to 1. Then, the iteration process of Equation (5) was begun to find an optimal matrix **S** in Equation (3). η in Equation (5) was 0.0001, and the number of maximum iterations was constrained to 200.

After constructing the optimal matrix **S**, $W(k)$ in Equation (1) of the cursor movement intents was estimated in real time by the matrix **S** times vector $M(k)$. Then, position of a control cursor (blue) was displayed using the joint synergy matrix in Equation (7) on the screen as shown in Fig. 2. In the three tests of each session, the subjects were asked to position the control cursor upon the target location. The target trajectories changed as shown in Fig. 4: (b) for the first test, (c) for the second test, and (d) for the third test. The trajectory in two dimensions for the first test is similar to the training stage. In the second test, the path of the trajectory was tilted by 45° with respect to the horizontal axis. To place the control cursor on the tilted trajectory, subjects combined multiple wrist movements among the four possible: wrist extension, wrist flexion, radial deviation, and ulnar deviation. In the third test, the horizontal line was repeatedly tilted by 0°, 30°, 60°, 90°, 120°, and 150° with respect to the horizontal axis. When the target was placed in the 0° or 90° tilted line, subjects did not need to combine multiple wrist movements as they did in the first test. In contrast, when the target was placed in the 30°, 60°, 120°, or 150° tilted line, subjects needed to combine multiple wrist movements as in the second test. Therefore, the third test was a combination of the first and second tests

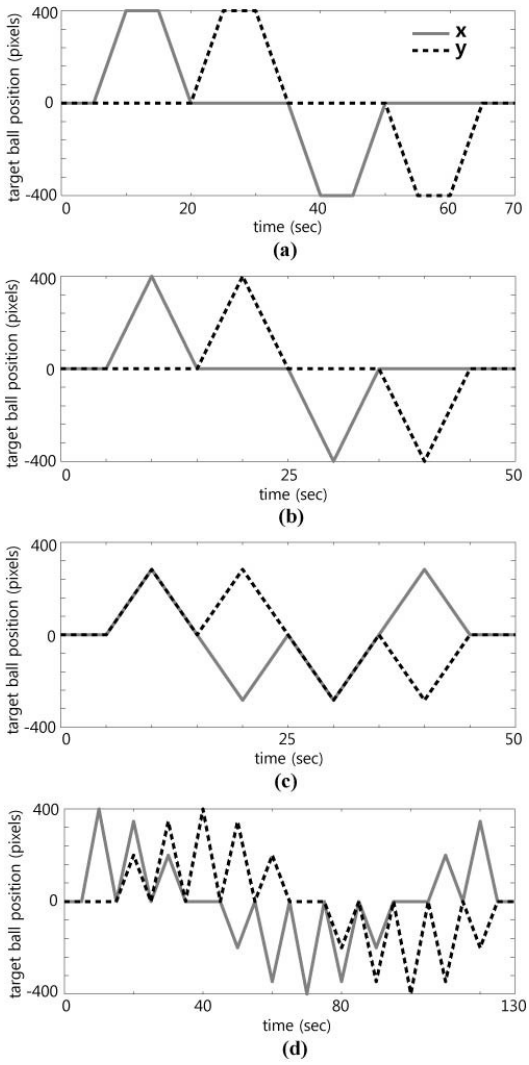

Fig. 4. Trajectories of a target cursor and its paths in the 2-dimensional space. Trajectory (a) was used for the training; trajectory (b), (c), and (d) were used for three tests.

IV. RESULTS

Figure 5 shows the convergence of the error based on the updated rules in Equation (5) with the non-negativity constraints to find the optimal matrix **S**, and the error converged to a fixed point within approximately 20 iterations.

Figure 6 shows graphical representations of muscle synergies averaged for each subject. Muscle synergies represent the muscle activations during wrist extension, wrist flexion, radial deviation, and ulnar deviation extracted by iterations of the updated rules. Each muscle synergy is represented as a bar graph across the six recorded muscles, and the vector magnitude was normalized to one. The synergies have a unique representation which involves an intuitive meaning of how much the activation of individual

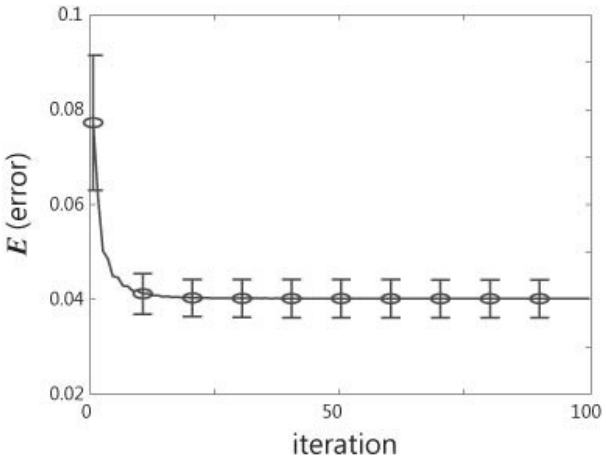

Fig. 5. Error convergence under the updated rules.

muscles affect individual wrist movements.

Figure 7 shows an example of the cursor tracking results via sEMG in a two-dimensional coordinate for three tests. It was evident that the subject could move a control cursor not only by wrist extension, wrist flexion, radial deviation, or ulnar deviation individually (first test), but also by combining them (second and third tests). TABLE I summarizes the estimation performances of the real-time experiment.

V. Discussions and Summary

The experimental results showed a great potential to develop a myoelectric joystick based on the wrist movements. Fluid wrist movements were extracted regarding a direction and its magnitude on a two-dimensional coordinate, and they provides the same information as a two-dimensional controller as a conventional joystick does. The myoelectric joystick is wearable and does not require a mechanically bulky frame. These facts are the most powerful motivations for the development of the myoelectric joystick.

This work could be extended to an alternative computer interface for individuals with the individual with transradial or wrist disarticulation level amputation. Limitations have been mentioned in the literature for applications specialized to the sEMG-based computer interface [5]. Those computer interfaces allow cursor movements restricted to only two directions (horizontal and vertical movements), and does not

TABLE I. R^2 (mean ± standard deviation) of the target cursor position relative to the control cursor position for each subject in the experiment.

	First Test	Second Test	Third Test
Subject A	95.56% ± 1.93	94.07% ± 4.52	94.48% ± 1.87
Subject B	91.10% ± 3.46	84.98% ± 8.20	87.35% ± 4.97
Subject C	88.24% ± 2.77	88.05% ± 3.29	89.07% ± 2.41
Subject D	92.13% ± 3.28	92.42% ± 2.15	92.86% ± 2.78
Subject E	96.00% ± 0.95	94.03% ± 2.14	94.13% ± 2.44
Average	**92.61% ± 3.38**	**90.71% ± 5.79**	**91.58% ± 4.16**

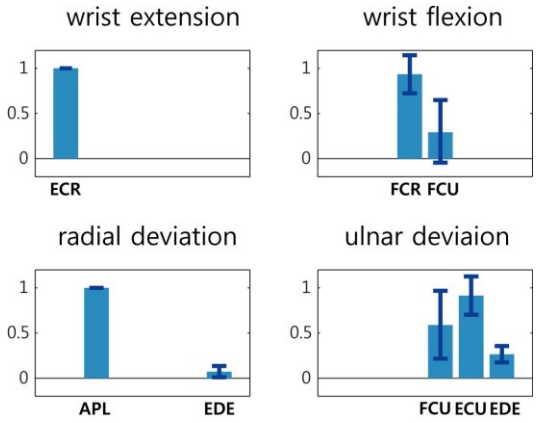

Fig. 6. Muscle synergies of Subject A are shown for wrist extension, wrist flexion, radial deviation, and ulnar deviation. Each muscle synergy is represented as a bar graph across the six recorded muscles, and the vector magnitude is normalized to one. Muscle synergies for the other subjects were not included here due to the limited length. We found that muscle synergies are different from all subjects.

allow movement in a diagonal direction. The suggested methods could improve accessibility of the computer by extracting the user intents to move the cursor not only horizontally and vertically but also diagonally.

This work is located in a line of research which seeks to develop a mapping model for multiple muscle activations to joint movements with multiple DOFs for myoelectric powered prosthetic wrists [17]. The non-negative muscle synergy matrix can map the relationship between multiple muscle activations and joint movements using only predefined movements (e.g., wrist extension, wrist flexion, radial deviation, and ulnar deviation), but can also express non-predefined movements (e.g., a combination of wrist extension and radial deviation). Although a muscle synergy concept has been involved in the previous researches [18], they have not been performed in real time. Our real-time

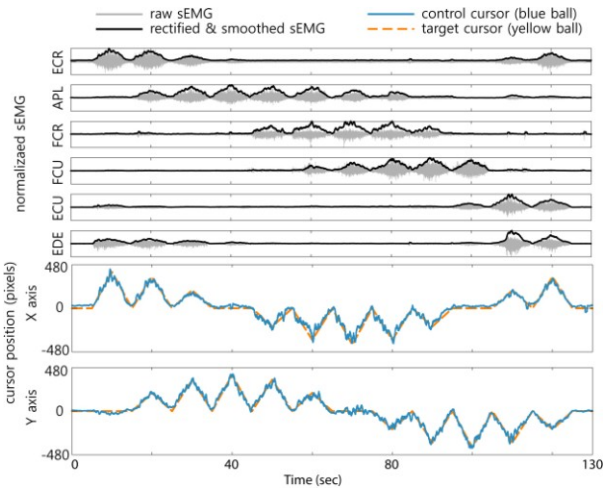

Fig. 7. Experimental results for the third test sessions. The upper graph shows raw sEMG and smoothed sEMG. The bottom graph shows positions of the target cursor and the control cursor.

implementation and validation of the algorithm with the muscle synergy matrix could be one step forward to actual clinical applications.

As shown in Fig. 6, the non-negative muscle synergy matrix enables visualization of the quantitative dependencies between multiple muscle activations and wrist joint movements. Even though previous research attempts have mapped muscle activations from sEMG to the wrist movements, these studies were performed using a machine learning algorithm [19-20], which has weak ability to obtain physiological meaning and whose internal parameters are difficult to interpret in contrast to the proposed matrix.

REFERENCES

[1] K. R. Wheeler and C. C. Jorgensen, "Gestures as input: Neuroelectric joysticks and keyboards," *IEEE Pervas Comput*, vol. 2, pp. 56-61, Apr-Jun 2003.

[2] C. Cipriani, F. Zaccone, S. Micera, and M. C. Carrozza, "On the shared control of an EMG-controlled prosthetic hand: Analysis of user-prosthesis interaction," *IEEE T Robot*, vol. 24, pp. 170-184, Feb 2008.

[3] P. K. Artemiadis and K. J. Kyriakopoulos, "EMG-Based Control of a Robot Arm Using Low-Dimensional Embeddings," *IEEE Trans Robot*, vol. 26, pp. 393-398, Apr 2010.

[4] C. Fleischer and G. Hommel, "A human-exoskeleton interface utilizing electromyography," *IEEE T Robot*, vol. 24, pp. 872-882, Aug 2008.

[5] C. Choi, S. Micera, J. Carpaneto, and J. Kim, "Development and Quantitative Performance Evaluation of a Noninvasive EMG Computer Interface," *IEEE Trans Biomed Eng*, vol. 56, pp. 188-191, Jan 2009.

[6] N. Bu, M. Okamoto, and T. Tsuji, "A Hybrid Motion Classification Approach for EMG-Based Human-Robot Interfaces Using Bayesian and Neural Networks," *IEEE T Robot*, vol. 25, pp. 502-511, Jun 2009.

[7] M. A. Oskoei and H. Hu, "Support vector machine-based classification scheme for myoelectric control applied to upper limb," IEEE Trans Biomed Eng, vol. 55, pp. 1956-65, Aug 2008.

[8] J. Li, Z. J. Wang, J. J. Eng, and M. J. McKeown, "Bayesian network modeling for discovering "dependent synergies" among muscles in reaching movements," *IEEE Trans Biomed Eng*, vol. 55, pp. 298-310, Jan 2008.

[9] J. U. Chu and Y. J. Lee, "Conjugate-prior-penalized learning of Gaussian mixture models for multifunction myoelectric hand control," *IEEE Trans Neural Syst Rehabil Eng*, vol. 17, pp. 287-97, Jun 2009.

[10] A. D. Chan and K. B. Englehart, "Continuous myoelectric control for powered prostheses using hidden Markov models," *IEEE Trans Biomed Eng*, vol. 52, pp. 121-4, Jan 2005.

[11] E. A. Clancy and N. Hogan, "Probability density of the surface electromyogram and its relation to amplitude detectors," *IEEE Trans Biomed Eng*, vol. 46, pp. 730-9, Jun 1999.

[12] E. Bizzi, A. D'Avella, P. Saltiel, and M. Tresch, "Modular organization of spinal motor systems," *Neuroscientist*, vol. 8, pp. 437-42, Oct 2002.

[13] A. d'Avella, P. Saltiel, and E. Bizzi, "Combinations of muscle synergies in the construction of a natural motor behavior," *Nat Neurosci*, vol. 6, pp. 300-8, Mar 2003.

[14] R. Merletti and P. Parker, Electromyography : physiology, engineering, and noninvasive applications. [Hoboken, NJ]: IEEE/John Wiley & Sons, 2004.

[15] Y. St-Amant, D. Rancourt, and E. A. Clancy, "Influence of smoothing window length on electromyogram amplitude estimates," *IEEE Trans Biomed Eng*, vol. 45, pp. 795-800, Jun 1998.

[16] T. D. Sanger, "Bayesian filtering of myoelectric signals," *J Neurophysiol*, vol. 97, pp. 1839-45, Feb 2007.

[17] J. U. Chu, I. Moon, Y. J. Lee, S. K. Kim, and M. S. Mun, "A supervised feature-projection-based real-time EMG pattern recognition for multifunction myoelectric hand control," *IEEE Trans Mechatron*, vol. 12, pp. 282-290, Jun 2007.

[18] N. Jiang, K. B. Englehart, and P. A. Parker, "Extracting simultaneous and proportional neural control information for multiple-DOF prostheses from the surface electromyographic signal," *IEEE Trans Biomed Eng*, vol. 56, pp. 1070-80, Apr 2009.

[19] C. Castellini and P. van der Smagt, "Surface EMG in advanced hand prosthetics," *Biol Cybern*, vol. 100, pp. 35-47, Jan 2009.

[20] J. J. Luh, G. C. Chang, C. K. Cheng, J. S. Lai, and T. S. Kuo, "Isokinetic elbow joint torques estimation from surface EMG and joint kinematic data: using an artificial neural network model," *J Electromyogr Kinesiol*, vol. 9, pp. 173-83, Jun 1999.